

Violent Star Formation in 30 Doradus

By R. C. KENNICUTT¹ AND Y.-H. CHU²

¹Steward Observatory, University of Arizona, Tucson, AZ 85721, USA

²Department of Astronomy, University of Illinois, Urbana, IL 61801, USA

The 30 Doradus nebula is the nearest example of a giant HII region, and as such it offers a unique laboratory for studying in detail the structure, stellar content, and dynamics of a starburst region. We begin with an overview of the 30 Doradus region on scales of 0.1–1000 pc, and then discuss two current problems of particular relevance to this conference, the stellar content and IMF in 30 Dor, and the violent dynamics of its interstellar medium.

1. Introduction

It is a pleasure to open a conference where 30 Doradus defines the *bottom* end of the star formation scale! The 30 Doradus region offers a most appropriate starting point for a conference on star formation in galaxies. It is the nearest example of a *bona fide* giant extragalactic HII region (GEHR), and it is the largest star forming region in the Local Group. It is large enough to exhibit many of the properties of the most luminous starbursts, yet close enough so that its physical structure and stellar content can be studied in detail. As such 30 Dor and other nearby GEHRs provide several crucial pieces of information about starbursts in general. They are the only regions where the embedded stellar population can be resolved and studied directly; this provides a unique stellar census of a starburst, which can be used to test the synthesis models which must be applied to more distant, unresolved GEHRs and starbursts. Imaging and spectroscopy of the gas provides a detailed picture of the physical conditions in the interstellar medium (ISM), hence these regions are the ideal laboratories for studying the complex dynamical interactions between massive stars and the surrounding ISM. Such feedback processes shape the large-scale structure of the ISM, and may well regulate the global evolution of galaxies. 30 Doradus offers all of the ingredients—a highly resolved concentration of thousands of massive stars in a dense, bright, dynamic, ionized medium—to serve as a “starburst Rosetta Stone” (Walborn 1991).

Excellent reviews of 30 Doradus have been published recently by Melnick (1987), Walborn (1991) and Meylan (1993), and we refer the reader to those references for a comprehensive review of recent work. In this paper we begin with a brief overview of the 30 Dor region (Section 2), then discuss two specific areas which are especially relevant to this conference, the stellar content and IMF in 30 Dor (Section 3) and the dynamics of its violent ISM (Section 4).

2. 30 Doradus as a prototype giant HII region

A useful definition of a giant HII region is any region which contains a sufficient number of massive stars so that its integrated spectra, physical properties, and evolution are dictated by the composite properties of its stellar population (e.g. total stellar mass, IMF, metallicity), rather than the individual properties of its most massive stars, or the local initial conditions in its parent star forming region. By this criterion 30 Doradus easily qualifies as a GEHR, because it contains so many stars that its IMF is fully populated to $\geq 100 M_{\odot}$. In this section we describe the 30 Dor region on different spatial scales, and compare it to other nearby star forming regions.

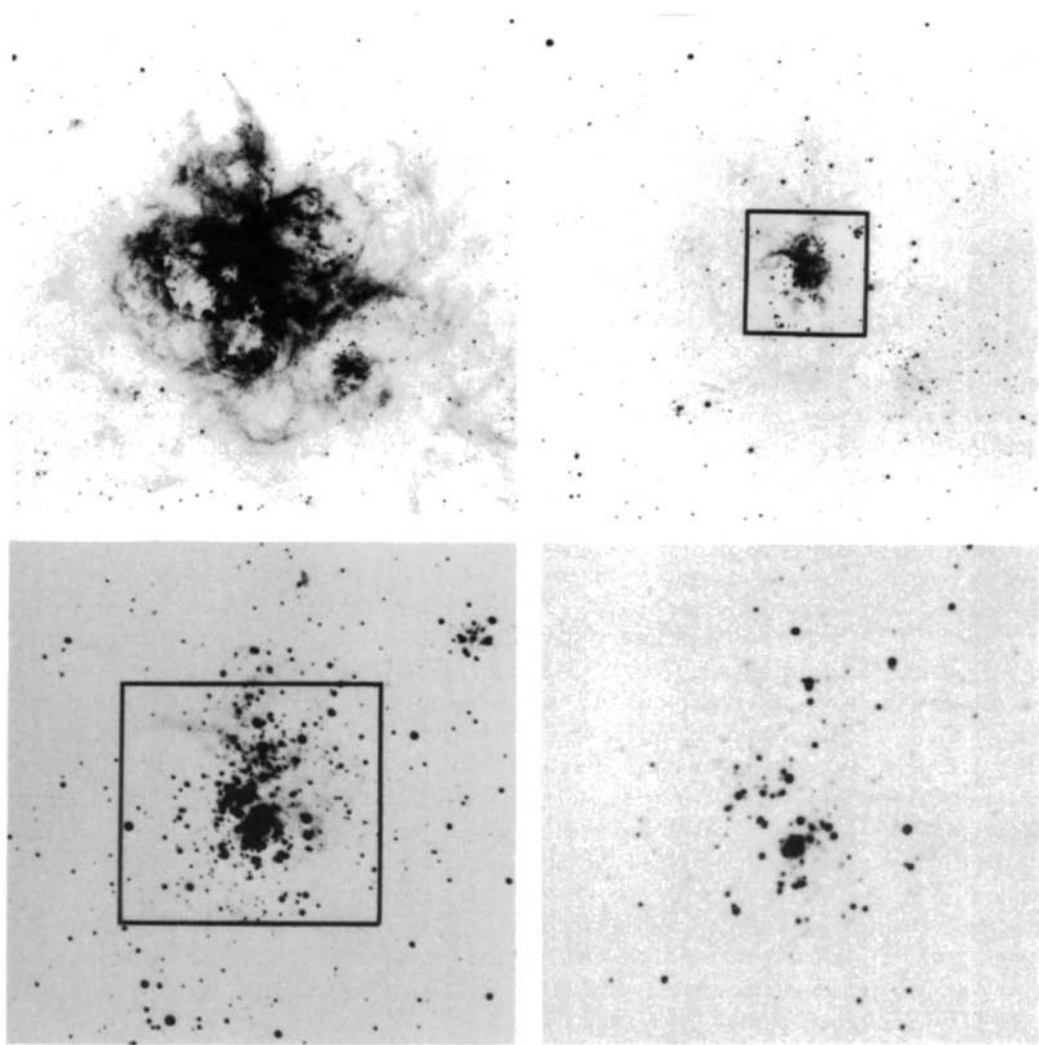


FIGURE 1. 30 Doradus and the star cluster NGC 2070. The top panels show a 23' (345 pc) region in $H\alpha$ and red continuum. The bottom panels are expanded photographs of the central star cluster. Boxes indicate the sizes of subsequent panels. From Kennicutt & Chu (1988).

2.1. Overview of the 30 Doradus region

Figures 1 and 2 show $H\alpha$ and continuum images of the 30 Doradus region on various scales. The central HII region (top panels in Figure 1) is roughly 15–20 arcmin or 200–300 pc across (assumed distance 50 kpc). Projected within the boundary of the nebula are several star clusters and associations, including the central cluster NGC 2070. Figure

2 is a deeper $H\alpha$ image of a 1600 pc region around 30 Dor, and it reveals that the nebula is located in the midst of a much larger superassociation. Two large HII/OB complexes, 30 Dor B (visible to the SE in Figure 1) and the supershell 30 Dor C, are located in the periphery of 30 Dor and are often considered to be part of the main HII region. Over 20 other large HII regions, OB associations, and star clusters surround this region, mostly to the south of 30 Dor. The ages of these stars range from 0 Myr (including obscured protostellar regions in N159 and 30 Dor itself) to 10–12 Myr (Melnick 1992). Two large expanding supergiant shells, LMC-2 and LMC-3, surround the eastern and western parts of the region, respectively (Meaburn 1980). A faint halo of $H\alpha$ emission envelops the entire 1 kpc region (Kennicutt & Hodge 1986); if observed from a large distance the whole complex might well be treated as a single supergiant HII region.

The picture of the 30 Dor region which emerges from these data is quite different from the simple single-age stellar population model which is usually applied to more distant GEHRs. Stellar photometry (e.g. Melnick 1987; Lortet & Testor 1991; Schild & Testor 1992; Parker 1993) shows that the region is actually a complex composite of several distinct stellar populations. Even the central nebula contains subclusters with ages ranging over at least 10 Myr. This means that the integrated spectrum of the region (or any similar GEHR) will be dominated by different stellar components at different wavelengths. While the emission-line spectrum of the photoionized gas will trace the youngest stellar population (<3 Myr), the underlying near-UV and visible continua may well be dominated by evolved supergiants from the older population (Searle 1971).

The bottom two panels of Figure 1 show enlarged views of the stars in the nebular core. The lower left panel (5.8 arcmin across) is comparable to the region which has been surveyed by Parker (1993), and contains over 2000 stars down to $V = 18$, not including the compact core cluster around R136. The bottom right panel shows the central 3 arcmin; the unresolved subcluster in the center is R136. It is interesting to note that at a distance of 15 Mpc the bottom panels in Figure 1 would subtend 1.2 and 0.6 arcsec, respectively! Even with the Hubble Space Telescope these regions are unresolvable beyond the Local Group. This emphasizes the importance of objects like 30 Dor for understanding the nature of starbursts on all scales.

2.2. Integrated properties and comparison with other objects

The integrated properties of 30 Dor were tabulated by Kennicutt (1984), and these provide a more quantitative picture of a prototypical GEHR. The extinction-corrected $H\alpha$ luminosity within a diameter of 370 pc is 1.5×10^{40} ergs s^{-1} , which corresponds to an ionizing luminosity of 1.1×10^{52} photons s^{-1} . The $H\alpha$ flux within $R < 4'$ (60 pc) is roughly 1/3 of this total, and is consistent with the ionizing luminosity expected from the ~ 2400 OB stars within that area (Parker 1992). The total mass of ionized gas in the nebula is roughly $8 \times 10^5 M_{\odot}$. These values are 2–3 orders of magnitude larger than well-known HII regions such as Orion, and several-fold larger than W49 and NGC 3603, the largest HII regions in the Galaxy (Kennicutt 1984). The difference between the LMC and Galactic populations is consistent with a general trend along the Hubble sequence. Although 30 Dor is unrivaled in the Galaxy, it is similar to the largest HII regions in other Magellanic irregulars of comparable mass, and several times less luminous than the brightest GEHRs in giant Sc galaxies such as M51 and M101 (Kennicutt 1988).

In addition to the differences in absolute scale, the physical conditions in the GEHRs are quite distinct from those in smaller, compact Galactic regions. The electron density ranges from ~ 100 – 300 cm^{-3} in the densest filaments to of order 1 – 10 cm^{-3} in the other parts of the nebula (Kennicutt 1984; Mathis, Chu, & Peterson 1985; Rosa & Mathis 1987). This compares to typical densities of order 10^2 – 10^4 cm^{-3} in compact HII

Cambridge University Press

978-0-521-47277-7 - Violent Star Formation: From 30 Doradus to QSOs

Edited by G. Tenorio-Tagle

Excerpt

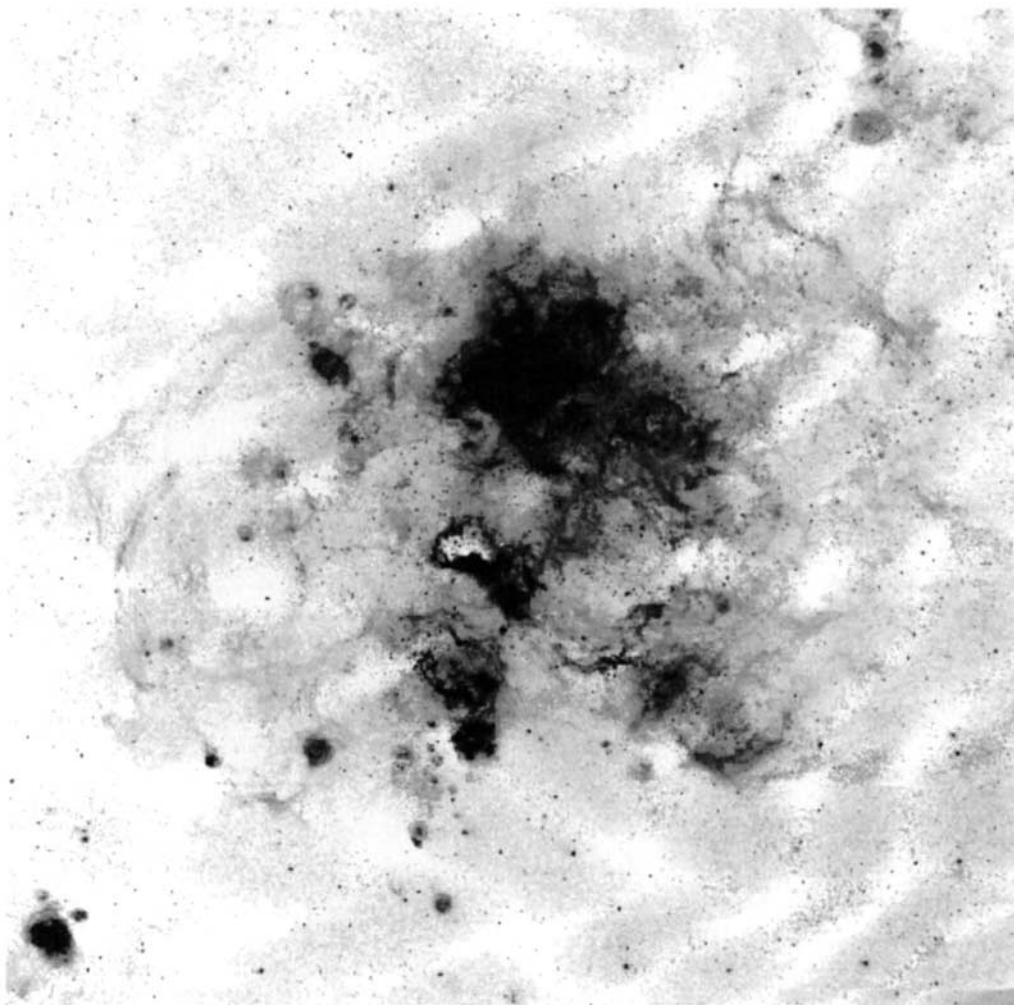
[More information](#)

FIGURE 2. $H\alpha$ image of the region surrounding 30 Dor, from Kennicutt & Hodge (1986).

regions. The visual extinction over most of 30 Dor is low, only 0–2 mag (Parker 1993; Dickel *et al.* 1994), though a few dusty condensations with protostars have been identified (Hyland *et al.* 1992). As will be discussed extensively at this conference, the ionized gas in GEHRs is much more turbulent, with supersonic velocity dispersions that are 2–3 times higher than in smaller HII regions. These differences are probably related to the concentration of massive stars, which facilitates the transfer of mechanical energy to the ISM from multiple stellar winds and supernovae. We return to this point in Section 4.

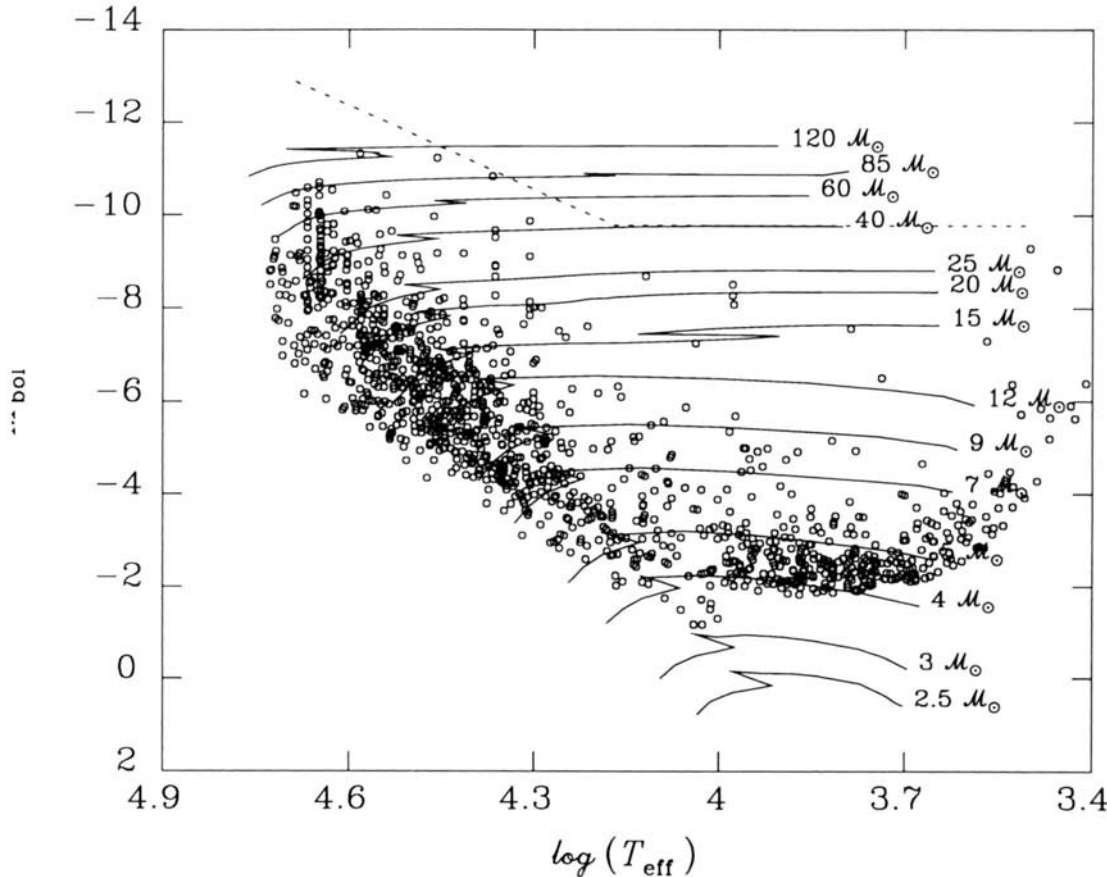


FIGURE 3. H-R diagram for the central 7' region of 30 Doradus, from Parker & Garmany (1993). Sample includes 1230 stars with low photometric errors.

3. Stellar content and IMF

As mentioned earlier the proximity of 30 Doradus provides a unique opportunity to measure the stellar population and the form of the initial mass function (IMF) in a starburst region. Numerous authors have resorted to various forms of biased IMFs—top-heavy IMFs, top and bottom-deficient IMFs, or bimodal IMFs—when attempting to account for the extraordinary luminosities of GEHRs and starbursts. The 30 Doradus region is an ideal testing ground for these biased IMF models. Ground-based *UBV* photometric surveys have been made by several investigators (Lee 1990; La Pierre & Moffatt 1991; Melnick 1992; Meylan 1993; Parker 1993), and HST observations of the core around R136 have been published by Campbell *et al.* (1992) and Malumuth & Heap (1994).

The most complete analysis to date is the thesis study of Parker. He surveyed a 50 arcmin² region in the center of 30 Dor, as part of a larger survey of the LMC by the Boulder group. CCD photometry in *UBV* was obtained for a complete sample of 2395 stars brighter than *B* = *V* = 18, and used to produce a reddening corrected H-R diagram. Classification spectra were obtained or compiled for ~140 stars brighter than *V* = 15.5, to provide accurate effective temperatures and bolometric corrections for the hottest and most massive stars. This provided a complete census of the upper end of the IMF for the

center of 30 Dor, except for a few Wolf-Rayet stars and the crowded region immediately around R136 (see below).

The final results of the analysis are summarized in Figure 3, which displays the H-R diagram for 1230 stars with the highest quality observations (Parker & Garmany 1993). Evolutionary tracks are superimposed on the data, and the present-day mass function can be derived simply by binning the stars in the respective mass intervals. Parker & Garmany find that the mass function above $12 M_{\odot}$ is well represented by a power law with slope $\Gamma \equiv d(\log N)/d(\log m) = -1.5 \pm 0.2$. If the cluster is younger than ~ 3 Myr, as appears to be the case, this PDMF represents the IMF in the region. The slope is considerably shallower than found for the solar neighborhood ($\Gamma = -2.2$) or the LMC outside 30 Dor ($\Gamma = -1.9$) by Blaha & Humphreys (1989), and it is shallower than the mean slope ($\Gamma = -2.0$) in 14 smaller LMC associations measured by Hill, Madore, & Freedman (1994).

Recent *HST* observations allow this analysis to be extended to the dense stellar core of 30 Dor, around the central object R136 (Campbell *et al.* 1992; Malumuth & Heap 1994). As reported by Malumuth at this conference, the IMF outside of R136 itself ($R > 3''.3$ or 0.8 pc) is consistent with the Parker and Garmany results ($\Gamma = -1.8$), but the slope becomes much shallower in the R136 core itself, with $\Gamma = -0.9$ for $R < 0.8$ pc (Malumuth & Heap 1994). For details we refer the reader to the paper by Malumuth & Heap in this volume.

These results taken together lend some support for a top-heavy IMF in GEHRs relative to smaller star forming regions. However it is interesting to note, as pointed out by Parker & Garmany, that previous measurements of the IMF in 30 Dor from *UBV* photometry (see references above) range over $\Gamma = -0.8$ to -2.0 in roughly the same region! Many of the existing data sets clearly are influenced by systematic errors, and complete homogeneous surveys are needed to test for systematic IMF variations, even in relatively accessible regions such as the Galaxy and the Magellanic Clouds. High-resolution infrared observations, which could extend the mass coverage from $\sim 10 M_{\odot}$ (the completeness level of most current surveys) to $\leq 1 M_{\odot}$ would be especially valuable (Zinneker 1994, this volume). As long as there is uncertainty in the IMFs determined for highly resolved GEHRs such as 30 Dor, any claims of anomalous IMFs in more distant, unresolved GEHRs and starbursts should be approached with a healthy degree of skepticism.

4. The Violent interstellar medium in 30 Doradus

The chaotic filamentary structure of 30 Doradus testifies to its violent internal dynamics. Early Fabry-Perot measurements revealed a supersonic velocity dispersion of 41 km s^{-1} FWHM, much higher than those for other HII regions in the Galaxy or Magellanic Clouds (Smith & Weedman 1972), while consistent with a general correlation between linewidth and nebular luminosity among GEHRs (Melnick 1977). High-resolution slit spectra resolved these motions into expanding shells on scales of $1\text{--}100$ pc (Meaburn 1984, 1988). The detection of several extended X-ray sources in 30 Dor by *Einstein* (Long, Helfand, & Grabelsky 1981; Chu & Mac Low 1990; Wang & Helfand 1991a) revealed hot gas which is presumably shocked by stellar winds and supernovae embedded in the nebula.

These observations point to a dynamical environment which is profoundly different from that in smaller HII regions. In a typical Galactic disk region massive stars form in relatively small associations, and at any particular location the time interval between successive Wolf-Rayet stars or supernovae is usually longer than the lifetime of an in-

Cambridge University Press

978-0-521-47277-7 - Violent Star Formation: From 30 Doradus to QSOs

Edited by G. Tenorio-Tagle

Excerpt

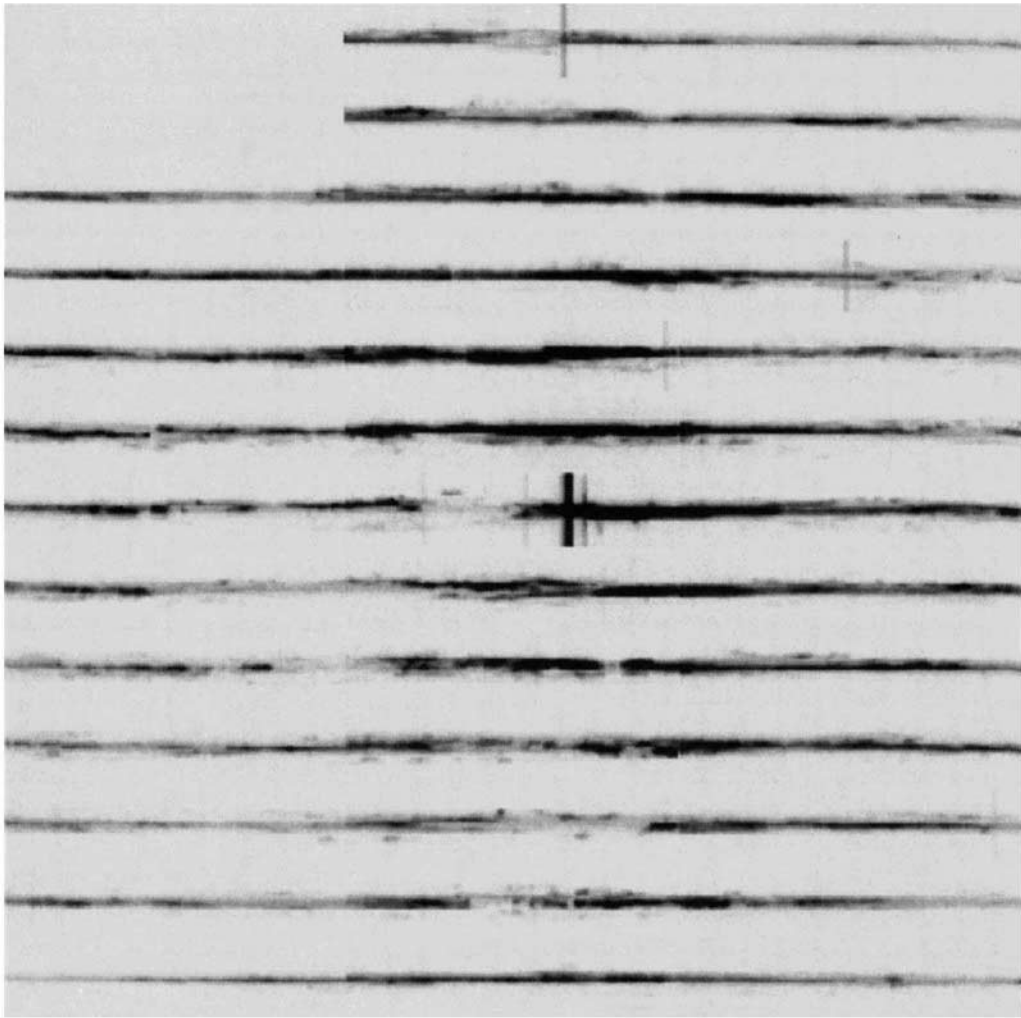
[More information](#)

FIGURE 4. Mosaic of 37 echelle line profiles in $H\alpha$, covering the central $9' \times 9'$ in 30 Doradus, from Chu & Kennicutt (1994). Orientation is N top, E left. Each $9'$ spectrum is separated by $45''$ N-S. Velocity range in each spectrum is $\pm 300 \text{ km s}^{-1}$. The continuum source near the center is R136.

dividual interstellar bubble or supernova remnant (SNR). In 30 Doradus the situation is dramatically different, with several hundred or thousand OB stars located within a radius of $\sim 1\text{--}20 \text{ pc}$. In such environments the surrounding ISM will be influenced by the collective stellar winds from the association, and subsequent supernovae will erupt within large wind-blown bubbles or previously formed SNRs. Such regions are the likely seed environments for the development of the large interstellar bubbles, supershells, and superwinds in galaxies. The ultimate effect of such a GEHR on its ambient ISM is likely to be quite different from an environment where the same number of massive stars are distributed in small, spatially isolated regions.

4.1. *Kinematic structure of 30 Doradus*

The 30 Doradus region offers a unique opportunity to study these collective interactions between massive stars and the ISM, and the early development of a supergiant shell. As part of a larger survey of the dynamics of the HII regions and SNRs in the Magellanic Clouds, we have mapped the kinematics of 30 Dor using the echelle spectrograph on the CTIO 4-m telescope in a single-order, long-slit mode (Chu *et al.* 1992; Chu & Kennicutt 1994). To illustrate the kinematics of the ionized gas in the central $9' \times 9'$ core, Figure 4 shows a mosaic of 37 E–W observations of the $H\alpha$ line, separated by $3'$ in the E–W direction and $45''$ N–S. The velocity range in each individual spectrum is $\pm 300 \text{ km s}^{-1}$. R136 is visible as the bright continuum feature near the center of the mosaic. Similar observations were obtained at 53 other positions outside the core. For several regions of interest, echellograms of the [SII] doublet were observed for shock diagnostics and density measurements.

The echellograms in Figure 4 reveal the extraordinary complexity of the violent motions in the center of 30 Dor. The outer parts of the HII region (mostly outside the region shown in Figure 4) are characterized by a relatively smooth velocity field, but with a much higher velocity dispersion than in other HII regions in the LMC. As one approaches the center of the nebula the velocity field becomes more complex, with multiple-velocity components at all positions. Several distinct types of kinematic features have been identified (Meaburn 1984; Chu & Kennicutt 1994). These include slow expanding shells with $V_{exp} < 100 \text{ km s}^{-1}$ and sizes from a few to $\sim 100 \text{ pc}$, and fast expanding shells with $V_{exp} = 100\text{--}300 \text{ km s}^{-1}$ and sizes from a few to $\sim 30 \text{ pc}$. There are also discrete high-velocity ($\Delta V > 100 \text{ km s}^{-1}$) features; some of them are isolated, while others are concentrated within large slow expanding shells, forming complex expanding networks. Several fast expanding shells and complex expanding networks are evident in Figure 4.

The slow expanding shells are commonly seen in other regions in the Galaxy or the Magellanic Clouds. The smaller objects ($\leq 15 \text{ pc}$) are probably stellar wind-blown bubbles, since the energetic requirements can be met with winds from one W-R star or a small number of OB stars. The larger slow shells (e.g. 30 Dor C outside the main nebula) can be accelerated by a combination of stellar winds and supernovae. The most massive of these, a 20 pc shell expanding at 40 km s^{-1} from the central star cluster, requires an impressive input energy ($\sim 10^{52} \text{ ergs}$), but this is not unreasonable given the concentration of massive stars in this region.

The fast expanding shells are the most spectacular kinematic features in 30 Doradus, and are only rarely seen elsewhere. No known wind-blown bubbles can match such high expansion velocities. The shell masses range from $100\text{--}5000 M_{\odot}$, and the kinetic energy in the visible ionized shells ranges over $10^{49} - 10^{51} \text{ ergs}$. The energy required to produce these shells, whether from stellar winds or supernovae, is roughly an order of magnitude higher, or $10^{50} - 10^{52} \text{ ergs}$. Stellar winds are a less plausible energy source for the fast shells, as the large energy requirement and short expansion ages ($10^4\text{--}10^5 \text{ yr}$) are usually inconsistent with the number of embedded stars. These fast shells most likely are SNRs inside 30 Dor.

The complex expanding networks are unique to 30 Doradus (within the LMC). Each network consists of a large slow expanding shell with additional high-velocity, shocked material within the shell boundary. This structure can be naturally explained by a wind-driven superbubble, with SNRs interacting with its shell walls. Chu & Mac Low (1990) have proposed the same mechanism to explain X-ray bright superbubbles in the LMC. Indeed, bright X-ray emission has been detected within the 30 Dor networks, as well as in the aforementioned fast shells.

4.2. *Soft X-ray properties of 30 Doradus and surroundings*

Soft X-ray observations are useful in tracing regions of fast shocks and delineating bubbles of hot gas in a large HII complex. We have obtained a *ROSAT* PSPC pointed observation of the 30 Dor region (Figure 5). The top panel shows the entire 30 Dor superassociation. The brightest sources are the X-ray binary LMC X-1, the known SNRs 30 Dor B and 0540-69.3, and two Galactic foreground stars. If the LMC were observed from a large distance these sources would be unresolved, and a significant fraction of the total flux would be contributed by LMC X-1 and the SNRs. Variable interstellar absorption at these low energies (0.1–2.4 keV) further complicates the analysis. This illustrates the difficulty inherent in interpreting X-ray observations of distant GEHRs and starbursts.

Figure 5b (bottom) shows a close-up, smoothed X-ray image centered on 30 Dor itself. Within 30 Dor, two types of X-ray sources are visible: point sources coincident with the stellar groupings R136 and R140, and extended diffuse emission associated with expanding shell structures. The fast expanding shells and networks identified in the echelle data have high X-ray surface brightness, while the shells without high-velocity features are much fainter in X-rays.

The diffuse X-ray sources in 30 Dor can be explained by SNRs interacting with pre-existing superbubbles (Chu & Mac Low 1990; Wang & Helfand 1991b). One such example is 30 Dor C, a superbubble around the OB association LH90; it has a limb-brightened shell structure in the X-ray image (Figure 5a). The SNR activity in 30 Dor C has been unambiguously confirmed by its nonthermal radio emission (Mathewson *et al.* 1985). A superbubble with SNRs interacting with its shell walls can emit 10^{35} to several times 10^{36} ergs s⁻¹ X-rays (Chu & Mac Low 1990; Chu *et al.* 1993). The diffuse X-ray emission from 30 Dor, at a level of $\sim 2 \times 10^{37}$ ergs s⁻¹ (Wang & Helfand 1991a), can be decomposed into 5–6 X-ray bright superbubbles (Chu *et al.* 1994, in preparation). The X-ray observations reveal the prevalent SNR activities in 30 Dor, but also illustrate that the 3-dimensional structure of 30 Dor is dominated by several large shells.

4.3. *Integrated kinematic properties*

We have used the uniform coverage of our echelle data in the central 9' core to estimate the total amounts of energy in the various types of velocity structures, and constrain the physical origin of the supersonic motions. When the echellograms in Figure 4 are summed to produce a single pseudo-integrated profile, the resulting profile has a remarkably smooth structure, as shown in Figure 6. This suggests that the roughly Gaussian velocity structure which is seen in the integrated profiles of more distant GEHRs (e.g. Melnick 1977) is not necessarily the result of virial motions, but rather is produced by the superposition of hundreds of smaller structures which are accelerated by a combination of stellar winds, supernovae, champagne flows, and truly turbulent motions.

A point-by-point analysis of the velocity field in the 30 Doradus core appears to support this conclusion (Chu & Kennicutt 1994). The background smooth turbulent velocity field is the largest single contributor to the total kinetic energy of the nebula, with $\sim 6 \times 10^{51}$ ergs. The high-velocity shells ($V_{exp} > 100$ km s⁻¹) and slower shells each contain approximately $3 - 4 \times 10^{51}$ ergs, with the shell around R136 alone contributing about 30% of the latter. It is interesting to note that although the high-velocity gas in 30 Dor contains a considerable fraction of the nebular kinetic energy, it represents an insignificant fraction of the integrated line emission. Most of the shells have emission measures of order $100 - 5000$ cm⁻⁶ pc, in contrast to $10^4 - 10^6$ for the foreground nebulosity. The total kinetic energy in the gas, $\sim 10^{52.2}$ ergs in the central 9', exceeds by at least an order of magnitude the gravitational binding energy of the complex, and suggests that most of 30 Dor, with the possible exception of the core star cluster, is literally blowing

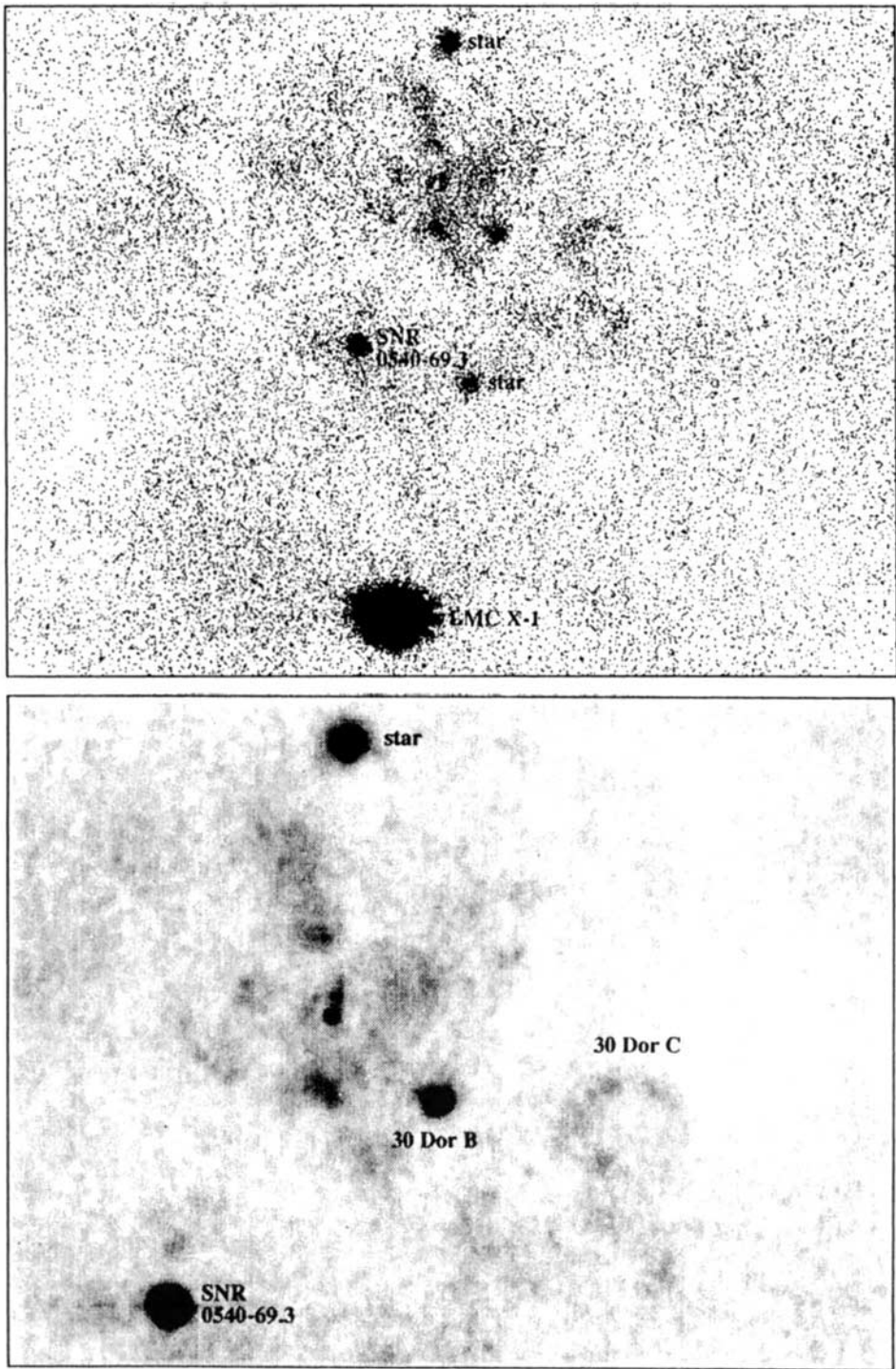


FIGURE 5. The 30 Doradus region as observed by the *ROSAT* PSPC. The top panel shows a $80' \times 60'$ field. The bottom panel is a smoothed expanded plot of 30 Dor itself, covering $42' \times 32'$. The point sources near the center are coincident with R136 and R140.